Site-specific recombination by the DDE family member mobile element IS*30* transposase

János Kiss, Mónika Szabó, and Ferenc Olasz†

Environmental Biosafety Research Institute, Agricultural Biotechnology Center, 4 Szent-Györgyi Albert Street, H-2100, Gödöllő, Hungary

Communicated by Werner Arber, University of Basel, Basel, Switzerland, October 8, 2003 (received for review June 17, 2003)

DNA rearrangements carried out by site-specific recombinases and transposases (Tpases) show striking similarities despite the wide spectrum of the catalytic mechanisms involved in the reactions. Here, we show that the bacterial insertion sequence (IS)*30* element can act similarly to site-specific systems. We have developed an inversion system using IS*30* Tpase and a viable λ phage, where the integration/excision system is replaced with IS*30*. Both models have been proved to operate analogously to their natural counterpart, confirming that a DDE family Tpase is able to fulfill the functions of site-specific recombinases. This work demonstrates that distinction between transposition and site-specific recombination becomes blurred, because both functions can be fulfilled by the same enzyme, and both types of rearrangements can be achieved by the same catalytic mechanisms.

It is now well documented that genetic information can be reshuffled by mobile elements that are usually distinguished as site-specific systems and transposons. Even though the output of their activity can be simplified to insertion, deletion, or inversion of DNA segments, transposition and site-specific recombination are generally regarded as distinct phenomena (1). Classification according to the protein-sequence motifs revealed that some transposases (Tpases) and site-specific recombinases (Recases) with entirely different functions fall within the same family (2–6). This finding supports that mechanistically dissimilar enzymes can perform similar biological functions and suggests that transposition and site-specific recombination may be closer to each other in some respect than was supposed earlier. Further support for this idea may emerge from insertion sequence (IS) elements that form an active junction composed of the inverted repeats (IRs) (7–10). This IR–IR junction shows similarities in its structure and function to the recombination sites of site-specific systems.

The *Escherichia coli* element, IS*30*, encoding a Tpase with the well conserved DDE signature (11), belongs to the increasing class of elements that transpose through an intermediate formed by abutted IRs (8). The IR–IR joint bracketing a 2-bp spacer is composed of the 26-bp left and right IR ends (IRL and IRR, respectively) that differ at three positions (12). IR–IR joints occur in both IS dimers and minicircles that can integrate into hot spot sequences or next to other IS*30* ends (13–15). Whereas transposition into a hot spot is a conventional way of translocation, which accompanies the resolution of IR–IR junction, targeting an IR end seems more specific for IS*30* and generates a new IR–IR joint. The IRs, together with the adjacent IS sequences, are important for the directionality of recombination, because, as always, IRL–IRR junction arises through dimerization or targeting an IR (8, 13, 16). The most frequent reaction has been observed when both donor and target DNA contain an IR–IR junction (13). In this case, the rearrangement is remarkably reversible and resembles site-specific recombination. Since joining the IRs and integrating the active junction next to an another IR seem to be highly site-specific activities, we decided to investigate whether IS*30* Tpase is able to act similarly to the known Recases.

Materials and Methods

Development of the Inversion and Deletion Systems and the Recombination Assay. Both pJKI106 and pJKI179 carry the Tn*5*-derived Km^R gene as a 1169-bp *Bgl*II–*Sal*I fragment, and the Tn*9*-derived Cm^R gene as a 773-bp *Taq*I fragment, both lacking their own promoters (17). The oppositely oriented genes are delimited by two junction fragments both composed of the 459-bp left and 106-bp right IS*30* ends separated by a GC spacer. Promoter activity of the right side junction was reduced by a TTG → GGT change at base pairs 1203–1205 of IS*30* applying the Kunkel method with the mutagenic oligonucleotide 5′-TTCAATCTG-TaccTGCAACACCC-3′. The mutation destroys the −35 promoter box in IRR (18). To prevent any expression from outside promoters, the $Sm^R\Omega$ fragment from pHP45Ω (19) carrying transcriptional and translational stop signals was inserted adjacent to the mutated junction.

Both plasmids were introduced into *rec*A⁻ HB101 (20) cells harboring the Tpase producer pJKI133 (15), and the transformants were incubated overnight on solid LB+Tc+Ap medium at 37°C. For negative controls, HB101 lacking pJKI133 was used, and the transformants were selected on LB+Ap. Plasmid DNA was extracted by the alkaline lysis method (21) from single colonies and digested with *Xho*I, which eliminated the Tpase producer plasmid. Digested DNA was transformed into *rec*A⁻ TG2 (21) cells and the Ap^R transformants were replica plated on LB+Km and LB+Cm to detect rearrangements. Plasmid DNA extracted from randomly selected Ap^R colonies was tested by digestion with *Eco*RI and *Pvu*II (pJKI106 ori① and ori②) or *Hin*dIII and *Pvu*II (pJKI179 and pJKI179Δ).

Construction of λPC Phages. To construct λ *red*⁻ ts cI Δ(*xis*, *int*, *att*P)::IS*30* Cm^R phages, the regions flanking the *xis*, *int*, *att*P segment were PCR-amplified and cloned. The 1.7-kb region preceding *att*P (base pairs 24797–26536) was amplified with the following oligonucleotides: 5′-CCAGTTCGCCGGGCAT-TCAAC-3′ and 5′-ttt*gtcgacgcggccgC*GCACGTGTGT-TAAATGGTTTGC-3′ and cloned as a *Hin*dIII–*Sal*I fragment including λ DNA from base pairs 25157–26536. The region upstream of the start codon of *int* (base pairs 28889–31941) was amplified with the following oligonucleotides: 5′-ata*ggatccctc-gag*TCCTCTTCAAAAGGCCACCTG-3′ and 5′-ACTTCCA-CACCCTGCTTGCTG-3′ and cloned as an *Eco*RI–*Bam*HI fragment comprising base pairs 28889–31747 of λ DNA [lowercase indicates non-λ-specific sequences carrying restriction sites (italics) used for cloning]. Both fragments were cloned in the Ap^R vector, pEMBL19 (22), in the correct orientation, and the IS*30*-Cm^R cassettes were inserted in between as *Xho*I–*Not*I fragments. PC349 carries a single Cm^R gene; PC365 contains the Cm^R gene followed by IS*30* from 63 to 1221 base pairs joined to the left end (1–169 base pairs) through a GC spacer. This construct comprises the full-length ORF of the Tpase from the

Abbreviations: IS, insertion sequence; IR, inverted repeat: IRL, left IR end; IRR, right IR end; Tpase, transposase; Recase, site-specific recombinase; TB, Tryptone broth.

†To whom correspondence should be addressed. E-mail: olasz@abc.hu.

www.pnas.org/cgi/doi/10.1073/pnas.2436518100

first base of the start codon (ORF-A: base pairs 63–1211), whereas in PC395, the ORF begins from a second in-frame ATG codon (ORF-A*: base pairs 180–1211), otherwise PC395 is the same as PC365. Due to the cloning design, the start codon of the ORFs is at the same position as ATG of λ *int* (base pairs 28882). Consequently, in the segment spanning base pairs 25157–31747 of λ DNA, the region of base pairs 26537–28888, including *att*P, the whole *int* and 3′ part of *xis* (overlapping with *int*) is replaced with the IS*30* and/or Cm^R gene cassettes.

The constructs were introduced into the λ genome by homologous recombination during lytic propagation of the λ *red*113 cI857 (a gift from H. Ikeda, Center for Basic Research, Kitasato Institute, Tokyo) in the *rec*A^+ TG1 strain (21) harboring one of the PC plasmids. This λ strain shows wild-type lysogenization at 30°C and is inducible at 37°C. The infected TG1 cultures were incubated at 37°C in Tryptone broth (TB) supplemented with 0.4% maltose and 10 mM $MgCl_2$ until complete lysis. Lysates were sterilized with chloroform and used to infect TG2 host at a multiplicity of infection (moi) of ≈ 0.1. Cultures were incubated 24–30 h on solid LB+Cm at 30°C. Colonies were selected according to the following criteria: only (*i*) small (<1 mm after 30 h incubation) Cm^R colonies that were (*ii*) Ap^S, (*iii*) unable to grow at 37°C on LB+Cm, (*iv*) caused either no or a small lysis spot on TG1 indicator bacteria at 30°C, and (*v*) gave lysis at 37°C. Colonies fulfilling these requirements were considered as potential abortive lysogens carrying double recombinant phage. Phages were recovered as individual plaques grown on indicator bacteria at inducing temperature. Several plaques were tested again for the ability of Cm^R transduction, lysogen (abortive) formation, and induction. Suitable phage clones were propagated on TG1 strain cultured in TB medium at 37°C until complete lysis, and then phage DNA was purified and their structure was confirmed by extensive restriction and PCR analyses. The structural integrity of the IS*30* components was proved also by sequencing. Restriction mapping and sequencing of λPC395 revealed a 5.5-kb deletion (base pairs 20301–25537) lying upstream from the replaced region and not affecting any essential λ genes.

Construction of *att*B_{IS30} Sites. For an attachment site (*att*B_{IS30}) for λPC phages, a junction composed of the truncated left (base pairs 1–169) and right (base pairs 1115–1221) IS*30* ends bracketing a GC spacer was inserted into the p15A-based plasmid pAW2015 (23) along with the $Sm^R\Omega$ fragment, resulting in the Km^RSm^R plasmid, pJKI373. TG2 strain harboring pJKI373 was the recipient host in the first lysogenization assay.

For developing a chromosomal *att*B_{IS30} site, the same junction was inserted into the Tn*10*-based Km^R minitransposon located on the Ap^R-conjugative suicide plasmid, pLOFKm (24). This plasmid was transferred by conjugation into TG2 and Km^RAp^S transconjugants carrying a single insertion of a mini-Tn*10* copy, but lacking donor plasmid backbone, were selected by virtue of Southern analysis. Insertion sites of the minitransposon were sequenced in several clones. One of these clones, TG2i4, carrying the insertion at the 314-bp position of *yhc*L gene (GenBank accession no. AAC76259) was used for chromosomal integration assays.

Lysogenization Assay and Microbial Characterization of Lysogens. TG2 cells harboring pJKI373 or the TG2i4 strain were grown overnight in TB+Km supplemented with 0.4% maltose and 10 mM $MgCl_2$ and infected with λPC395 at an moi of ≈ 0.01–0.05. Cells were spread onto LB+Cm plates and incubated 18–20 h at 30°C (only integrant lysogens form colonies during this time). For screening the potential lysogens, ≈50 normal-sized Cm^RKm^R colonies were individually tested on LB+Cm and on indicator bacteria at 30 and 37°C. The integrant lysogen forms a colony on Cm at 30°C after 20 h incubation ($Cm30^+$), whereas, at 37°C, no colony is formed due to the induction of the lytic cycle of the phage ($Cm37^-$). The ability of phage production was tested on the phage-sensitive indicator strain, TG1. At the noninducing temperature, either no lysis spot, or a small lysis spot, is formed around the lysogen colony transferred to the lawn of indicator bacteria, indicating the correct repression of the phage ($\phi30^-$). Conversely, the same colony produces a large lysis spot at 37°C, indicating the production of viable phage particles ($\phi37^+$). The $Cm30^+$-, $Cm37^-$-, $\phi30^-$-, and $\phi37^+$-stable lysogen colonies were selected for further analyses by a microbial test where the proper clones were streaked for single colonies and at least 20 were individually tested for the original $Cm30^+$, $Cm37^-$, $\phi30^-$, and $\phi37^+$ phenotype.

Analysis of Integration and Excision of λPC395 in pJKI373. To verify the integrant lysogenic state, total DNA was isolated (15) from the colonies that provided positive signals for the *att*L_{IS30} and *att*R_{IS30} junctions in colony PCRs. Templates in colony PCRs were single colonies suspended in distilled water, the primers and cycling conditions were described as follows: The DNA was transformed into TG2 cells harboring a helper plasmid that expressed the λ repressor (ts cI857) to stabilize the lysogen status of the transformants. Total DNA was isolated from the Km^R, $Cm30^+$, $Cm37^-$, $\phi30^-$, and $\phi37^+$ transformants grown overnight at 30°C in TB+Km+Cm and amplified with four primer combinations. The primers used were as follows: a-b for *att*B_{IS30}, c-d for *att*P_{IS30}, a-d for *att*L_{IS30}, and c-b for *att*R_{IS30} (a, 5′-GAGCTGAATGAAGCCATACCAAACGAC-3′; b, 5′-GATGTTACCCGAGAGCTTGGC-3′; c, 5′-CAGCTCACCGTCTTTCATTGC-3′; and d, 5′-GACATCTAGAATTTACTGTCA-3′).

To examine excision, a single lysogen colony was grown overnight at 30°C in TB+Km+Cm, and the culture was then diluted to ≈10^8 cells per ml and incubated at 37°C under vigorous shaking. Samples were taken in every 10 min, phage titer was determined, and total DNA was isolated and analyzed by PCR as described above.

Integration and Excision Assays in the Genomic *att*B_{IS30} Site. Genomic DNA purified from the potential lysogens (phenotype: $Cm30^+$, $Cm37^-$, $\phi30^-$, and $\phi37^+$) was amplified with the following primer combinations for detecting junctions: e-f for *att*B_{IS30}, c-d for *att*P_{IS30}, e-d for *att*L_{IS30}, and c-f for *att*R_{IS30} (e, 5′-TATCTTGTGCAATGTAACATCAGAGA-3′; and f, 5′-tgaattcATAATATACGGCGAGCGAATGAG-3′. Primers c and d were the same as in previous experiment). The phage induction assay with the TG2i4::λPC395 lysogens was carried out as described above. For detection of *att*P_{IS30} and *att*B_{IS30}, the same primer combinations were used as in the test of lysogens.

Results

Site-Specific Inversion by IS*30* Tpase. We have constructed an inversion model system that is structurally analogous to the invertible G segment of bacteriophage, Mu (Fig. 1*A*). In the model plasmid, the IR–IR joints having similar symmetry to those of *gix* sites (25) served as recombinogenic sequences, whereas IS*30* Tpase was expressed from a compatible plasmid (see *Materials and Methods*). The resistance genes bracketed by the inversely oriented IR–IR joints could be expressed from the promoters located in the IRs (18). To avoid coexpression of both marker genes, one of these promoters has been destroyed by point mutations, so the expressed resistance marker refers to the actual orientation of the segment. The original construct providing high level of Km^R (ori①) was introduced into *rec*A^- *E. coli* cells harboring the Tpase producer, then plasmid DNA was isolated and transformed again to sort out the rearranged species as individual clones. Among 30 randomly selected transformants, one showed a high level of Cm^R and turned out to carry

GENETICS

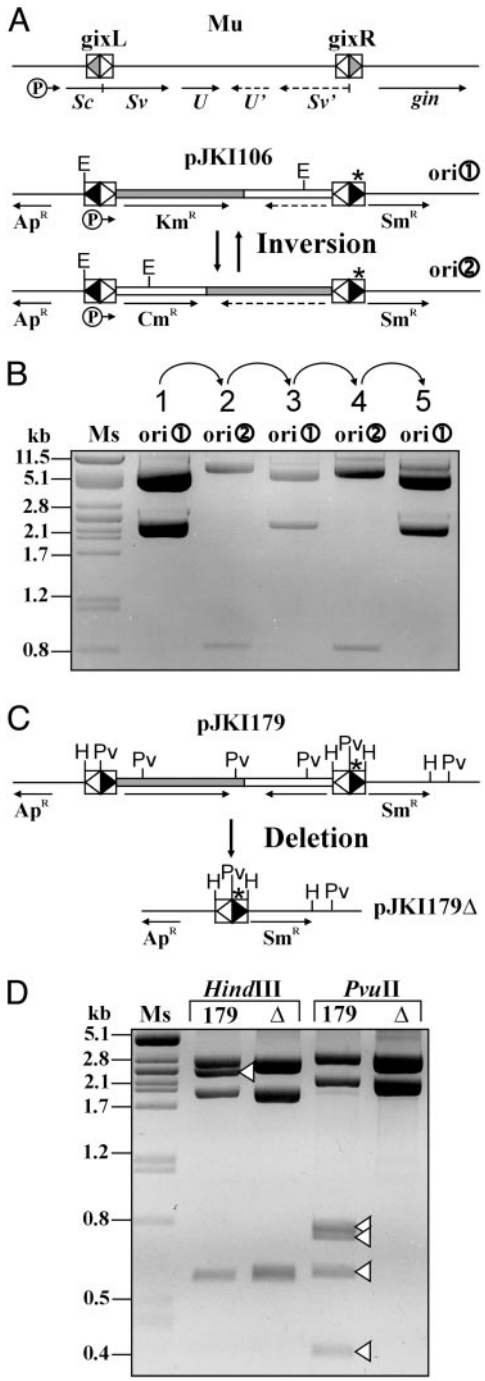

Fig. 1. Inversion and deletion occurring between two IS*30* IR–IR joints. (*A*) The invertible segment of pJKI106 and its structural and functional analogy to the G segment of bacteriophage Mu (25). Arrows and dashed arrows refer to expressed and nonexpressed genes, respectively, and ''P'' marks the promoters. Differently shaded triangles within boxes indicate the symmetric recombinogenic sites. The IS*30*-based inversion system contains the promoterless Km^R (shaded box) and Cm^R (white box) genes bracketed by two inversely oriented IR–IR junctions that act as recombination sites. The white and black triangles refer to the IRL and IRR of IS*30*, respectively. *, the inactivated promoter in the right side junction (see *Materials and Methods*); E, *Eco*RI. (*B*) Consecutive inversions. Plasmid DNA exposed to Tpase was digested with *Eco*RI. Lane 1, original pJKI106; lanes 2–5, plasmid DNA having undergone inversion during consecutive passages. Each isolate derives from that shown in the preceding lane. Ms, λ DNA cleaved with *Pst*I. (*C*) Deletion occurring between IR–IR joints arranged in direct orientation in pJKI179. H, *Hin*dIII; Pv, *Pvu*II. (*D*) Comparison of pJKI179 and its site-specific deletion derivative, pJKI179Δ. Deleted fragments are indicated.

an inversion (ori②). The inversion plasmid was reintroduced to the Tpase producer strain and analyzed again. In two parallel experiments, 28 of 75 and 19 of 30 colonies, respectively, contained the segment in the original direction (ori①). The next passage provided 8 of 30 and 2 of 30, whereas the last one yielded 1 of 20 and 4 of 20 inversions (Fig. 1*B*). Both ori① and ori② structures failed to undergo inversion (0 of 60) in similar experiments performed without Tpase producer. All constructs described carry a GC spacer in the IR–IR junction, which, together with the first two bases of the IRs, results in a *Pvu*II restriction site. This result provides a simple and informative assay to test whether base changes occurred in the rearranged junctions during recombination (13). Analysis of the junctions by *Pvu*II digestion confirmed that each inversion occurred without any base change in the recombinogenic sites.

In addition to inversions (23% of the 235 analyzed events), two types of other reactions were also observed. One of them was the intermolecular recombination through two IR–IR junctions, resulting in dimer replicons (44%). This reaction showed the same conservative site-specific manner as did inversions. The apparently high frequency of dimerization may derive from the replication advantage of dimer replicons (26), which considerably distorts the estimation of the real contribution of dimerization in the rearrangements. The other was the intramolecular transposition leading to deletion formation (20%), where one of the IR–IR junctions targeted a non-IR sequence in the plasmid. In the remaining 13% of cases, alterations could not be detected.

To examine whether outcome of the reaction (i.e., inversion or deletion) depends on the relative direction of IR–IR joints, we constructed a plasmid that differed from the inversion model only in the direct orientation of the junctions (Fig. 1*C*). This plasmid exposed to Tpase frequently produced site-specific deletion removing the Cm^R and Km^R marker genes along with one of the IR–IR junctions (90–95%), whereas the frequency of deletions was <0.1% in absence of Tpase (Fig. 1*D*). Other types of rearrangements were not observed and the remaining 5–10% of the analyzed clones were the same as the original structure. This site-specific behavior was strikingly similar to that of resolution systems, where the recombination occurs between two directly repeated resolution sites [e.g., two *lox*P or *dif* sites (27, 28)]. Conspicuous absence of inversions in case of directly oriented junctions (pJKI179) and, conversely, the absence of pJKI179Δ-type deletion products in the inversion model clearly showed that the orientation of the recombinogenic sites defined the product of recombination. Further analyses confirmed that the reaction between two IR–IR junctions was conservative, site-specific, and frequent enough to be applied in another recombination system that is closer to a natural situation.

Replacement of the λ Integration/Excision System by Components of IS*30*. We assessed whether IS*30* Tpase, along with the appropriately positioned junctions, was able to substitute for the site-specific recombination system of phage λ. A *red*$^-$ ts cI λ strain was used for replacing its *int-att*P region with the Tpase gene and an IR–IR junction ($attP_{IS30}$). Thus, the recombinant phage did not contain any components of the original site-specific system. In addition, Tpase expression was placed under the control of λ cI repression. Three types of phages were used in the integration assays (see *Materials and Methods*), where an IR–IR junction located on a plasmid served as an attachment site ($attB_{IS30}$). λPC349 carried a Cm^R gene alone, λPC365 and λPC395 further contained an IRL–IRR junction and a coding sequence of a full or an N-terminally truncated IS*30* Tpase, respectively (Fig. 2*A*). A *rec*A$^-$ *E. coli* strain harboring pJKI373 (Fig. 2*B*) was infected with λPC349, λPC365, or λPC395, and the potential integrant lysogens were selected for the Cm^R phenotype. Neither λPC349 nor λPC365 produced stable Cm^R lysogens, and integration into pJKI373 was never detected. The latter phage turned out to be

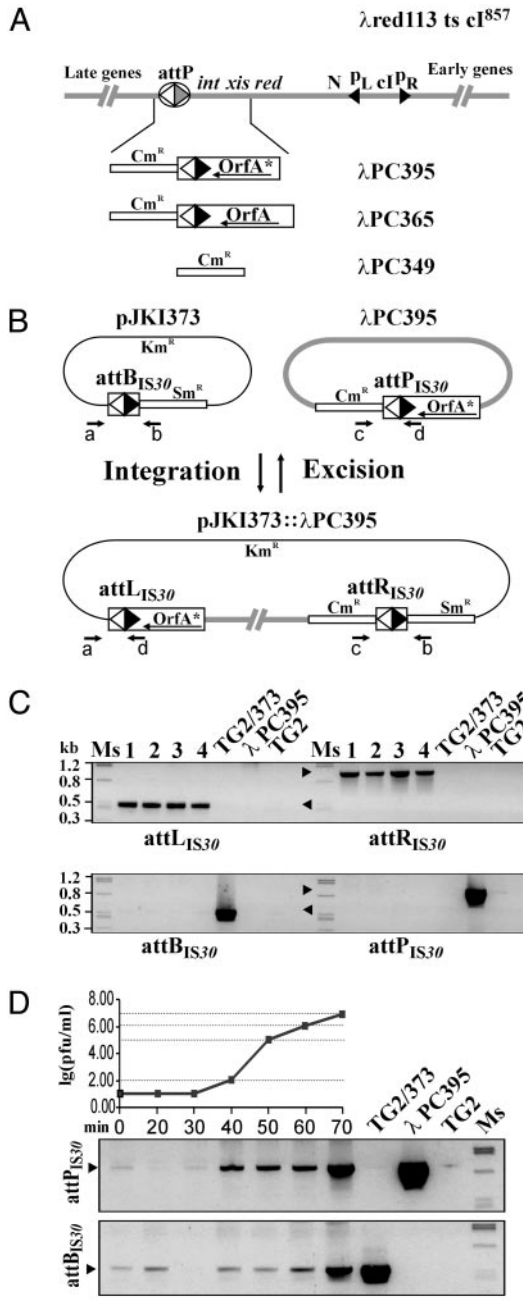

Fig. 2. Integration and excision of λPC395. (*A*) A schematic map of λ (35) and the IS*30*-based systems that substitute its site-specific system. λPC395, λPC365, and λPC349 carry the shortened IS*30* ORF-A* (amino acids 40–383), the whole ORF-A, or the Cm^R gene alone, respectively. (*B*) Integration and excision of λPC395 in the target plasmid, pJKI373. Thin line, plasmid backbone; thick line, λ DNA; open boxes, resistance genes as indicated; black and white triangles, IR–IR junctions designated as *att* sites according to their location. Primers used for detecting *att* junctions are indicated as a–d (see *Materials and Methods*). (*C*) PCR detection of integrated λPC395. Samples 1–4 (independent isolates) gave no signal for $attB_{IS30}$ and $attP_{IS30}$ (arrowheads), but yielded PCR products indicative of $attL_{IS30}$ (base pairs 500) and $attR_{IS30}$ (base pairs 940). TG2/373 and λPC395, positive controls for $attB_{IS30}$ (base pairs 534) and $attP_{IS30}$ (base pairs 890); TG2, negative control. (*D*) Excision of λPC395 during induction of a lysogen strain. The excision was assayed by titration of phages and PCR detection of $attB_{IS30}$ and $attP_{IS30}$ every 10 min. Control PCRs for $attB_{IS30}$ and $attP_{IS30}$ were as in *C*.

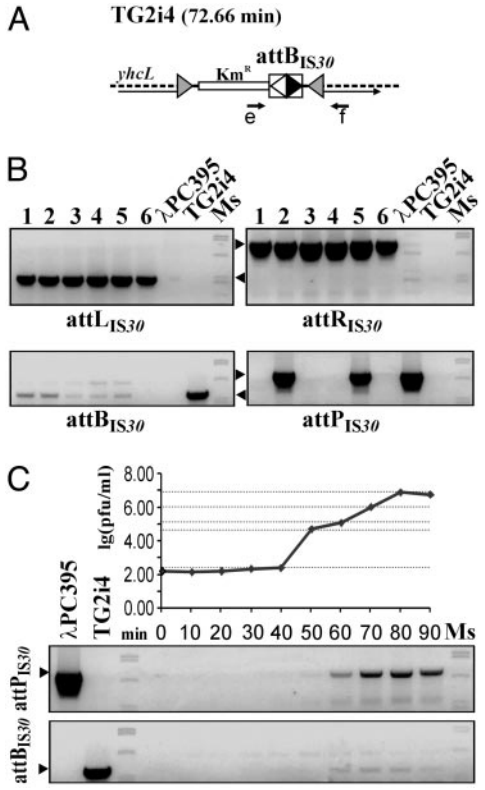

Fig. 3. Integration and excision of λPC395 in the chromosomal $attB_{IS30}$ site. (*A*) Location of the integrated $attB_{IS30}$ in the *E. coli* genome. The shaded arrowheads bracketing the Km^R gene with the IS*30* IR–IR junction represent the ends of Tn*10* minitransposon (see *Materials and Methods*). Thin arrow, *yhc*L gene; e and f, primers used in PCRs. (*B*) PCR analysis of six integrant lysogens. Lanes 1–6 show the amplification products obtained with the primer combinations of e–f for $attB_{IS30}$ (base pairs 571), c–d for $attP_{IS30}$ (base pairs 890; see Fig. 2*B*), e–d for $attL_{IS30}$ (base pairs 512), and c–f for $attR_{IS30}$ (base pairs 943). The weak $attB_{IS30}$-specific signals suggest that these clones showed spontaneous excision similarly to a wild-type λ lysogen. Positive signals for $attP_{IS30}$ in lanes 2 and 5 may also be derived from imperfect phage repression. (*C*) Excision of λPC395 during lytic phase of a lysogen. The excision was assayed by titration of phages and PCR detection of $attB_{IS30}$ and $attP_{IS30}$.

quite unstable and produced various Cm^S deletion derivatives. However, this instability was not surprising as the wild-type Tpase has many known hot spots in λ DNA that may contribute to the decay of the phage (14). Conversely, λPC395, which expressed a shortened Tpase lacking the first 39 amino acids, which is defective in hot spot recognition (Z. Nagy, personal communication) yielded stable Cm^R lysogens (Fig. 2*B*). From three parallel infections, four of 40 Cm^R-stable lysogen colonies showed positive signal in colony PCR for $attL_{IS30}$ and $attR_{IS30}$ junctions. The pJKI373::λPC395 fusion products from these clones were transformed into a host expressing the cI repressor to stabilize lysogen transformants. Subsequent analyses of colonies obtained confirmed that $attL_{IS30}$ and $attR_{IS30}$ were present, whereas $attP_{IS30}$ and $attB_{IS30}$ were missing from the cointegrates (Fig. 2*C*). Sequencing of junction fragments also confirmed that λPC395 integrated into the $attB_{IS30}$ site in a conservative and site-specific manner. The dynamics of the reverse process, the excision of the phage, was also investigated (Fig. 2*D*). During induction of a lysogen, the temporal change of both the phage titer and the relative intensity of $attP_{IS30}$- and $attB_{IS30}$-specific PCR fragments indicated the correct excision. Sequencing the PCR fragments also confirmed their identity to the original junctions.

Genomic Integration and Excision of λPC395. Approaching this model system to the natural situation, the $attB_{IS30}$ site was inserted into the host chromosome, yielding the TG2i4 strain

Table 1. Comparison of the properties of site-specific, transpositional, and IS*30* IR–IR-mediated recombination

Characteristics	Site-specific recombination	(IR–IR) × (IR–IR)	Transposition
Mechanism	Conservative	Conservative	Conservative or replicative
Frequency of recombination	High	High	Low
Specific sequence requirements on			
Donor DNA	Yes (*res, dix, att, lox, dif*)	Yes (IR–IR)	Yes (IR)
Target DNA	Yes (*res, dix, att, lox, dif*)	Yes (IR–IR)	Variable specificity
Target site after recombination	Unaltered	Unaltered	Duplicated or unaltered
Host factors	None or IHF, HU, FIS, etc.	None	None or IHF, HU, FIS, etc.
Catalytic motif involved*	Active Ser/Tyr, DED/DDD,	DDE	DDE, active Tyr, DED/DDD

*Active Ser, Invertase/resolvase family; active Tyr, integrase family; DED/DDD, Piv/Moov/IS*110* family; DDE, transposase/retroviral integrase family.

(Fig. 3*A*), which was used to test the ability of λPC395 to integrate into a single $att\mathrm{B}_{\mathrm{IS}30}$ site embedded in the 4.6-Mb *E. coli* genome. TG2i4 cells were infected with λPC395 and the lysogens were selected for the stable Cm^{R} phenotype. PCR analyses confirmed that 6 of 22 colonies selected from three parallel experiments according to phenotype tests (see *Materials and Methods*) carried the phage integrated into the $att\mathrm{B}_{\mathrm{IS}30}$ site (Fig. 3*B*). The remaining 16 clones were also stable Cm^{R} lysogens, where the PCR test could not detect $att\mathrm{P}_{\mathrm{IS}30}$ but could detect $att\mathrm{B}_{\mathrm{IS}30}$, suggesting that the integration in these cases occurred elsewhere in the genome. The strong lysis and the very low final titer ($<10^4$ cfu/ml) produced by these clones under inductive circumstances also supports that the integrant phage could poorly excise from non-*att*B sites.

The lytic phase of the phage integrated into the $att\mathrm{B}_{\mathrm{IS}30}$ site was examined as previously. In the course of phage induction assay, the temporal increase of phage titers from 10^2 to 10^7-10^8 pfu/ml, the gradual increase of the indicative PCR fragments (Fig. 3*C*), and the following sequence analysis of the restored $att\mathrm{B}_{\mathrm{IS}30}$ and $att\mathrm{P}_{\mathrm{IS}30}$ sites all supported that the phage correctly excised and propagated. Conversely, in a similar experiment where λPC395 had been integrated into a secondary (non-IR) site, the maximal titer did not exceed 10^3 pfu/ml during induction. This result clearly showed that effective excision required the recombination between intact $att_{\mathrm{IS}30}$ sites.

Discussion

In this work, we provide evidence that an enzyme belonging to the DDE family of Tpases can act as a site-specific Recase. The model systems described here fulfill the same functions as the well known site-specific inversion, resolution, or phage integration/excision systems. For such functions of IS*30* Tpase, only three constraints are required: (*i*) the joined IRs are the reactive sites (8), (*ii*) the IRs (even more, the IR–IR junction) are preferred sites for integration (13), and (*iii*) the left and right ends of the element can be distinguished (8, 13). The last criterion is needed for determining the issue of intramolecular recombination. The relative orientation of the reactive sites prescribes that inversion or deletion will occur (Fig. 1). In the natural systems, the orientation of recombination sites has similar determinative function (29–31), although accessory functions have evolved in many cases to restrict the secondary activities [e.g., FIS enhances inversion by Gin-invertase (32)].

The known site-specific systems show many analogies with those based on IS*30* (Table 1), indicating that certain transposons might have served as starting points for the evolution of site-specific systems. IS*30* seems not exceptional in this respect. Accumulating data suggest that numerous IS elements may suit the above requirements (7, 9, 10, 33). Mutations such as deletions removing almost an entire element from the dimer, but leaving the IR–IR junction intact or eliminating the domain of Tpase involved in target selection, might easily establish the primitive form of a new site-specific system (Fig. 4*A*), which can improve further in the course of evolution. It is worth noting that the reverse scenario (i.e., establishment of a new transposable element based on a site-specific system) is also possible (Fig. 4*B*). Truncated IS*30* Tpase carries out secondary reactions similarly to natural systems: Ser-invertases cause deletion or cointegration (30, 31, 34) and λ can integrate into secondary sites (35). More accurate functioning can be achieved by natural selection, as shown in the presented model (Fig. 4). λPC395 could not efficiently excise from secondary sites, therefore, those integrants produced orders of magnitude fewer phage particles during the lytic cycle. Thus, their extinction is more probable in the course of evolution.

It is now clear that covalent protein-DNA intermediate formation is not an exclusive criterion of site-specific recombination. The same recombination function can be fulfilled by enzymes with divergent enzymatic mechanisms such as inversion by Ser-Recases, Tyr-Recases, or Piv, which is rather related to Tpases (3). Conversely, the same molecular mechanism can be applied to different functions (Table 2) such as inversion, resolution, integration, excision, or transposition, as is seen in the Int family (5). Here, we demonstrate the ability of a DDE Tpase

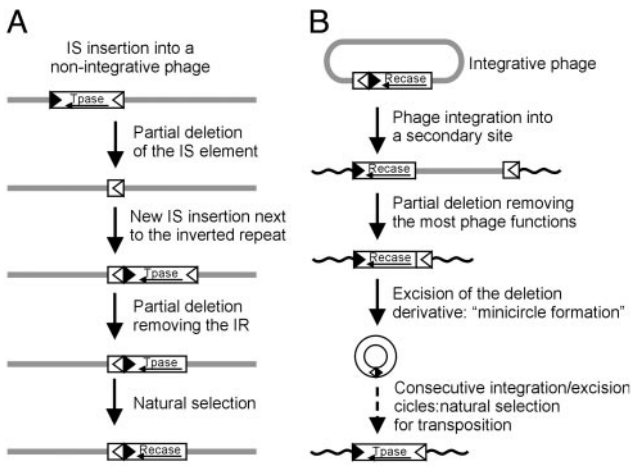

Fig. 4. Hypothetic possibilities for the evolution of a site-specific and a transposition system from each other. (*A*) A possible sequence of events potentially leading to the spontaneous development of a phage-encoded site-specific recombination system based on a transposable element. Most of these steps have already been described in different systems [IS insertion into a phage (36), partial deletion of an IS (37), and insertion adjacent to an IR (15)]. This series of events is only one of the numerous conceivable scenarios. Note that the third state is already able to fulfill the site-specific integration and excision by using an IR end as *att* site (13). (*B*) The reverse process resulting in a transposon is also possible. Note that the phage integrated into a secondary site is structurally analog to a transposon. Thick line, phage DNA; curved line, DNA of the host cell; black and white arrowheads, IRs; open box, coding sequence of the recombinase.

Table 2. Functional classification of some well known recombinases

Family	Catalytic motif	Functional classification of recombinases: Transposase	Invertase	Resolvase	Viral integrase	Integron integrase	V(D)J recombinase	Ref(s).
Integrase	Active Tyr	Tn*916*, Int, Tn*554*, Tnp A, B	Fim B, E, Flp	Cre, Xer C, D, Tn*4430* TnpI	λ Int, P22 Int, ϕ80 Int	Tn*21* Int 11, Tn*7* Int 12	—	5
Invertase/ resolvase	Active Ser	—	Bin, Cin, Gin, Hin, Min, Pin	Tn*3* TnpR, $\gamma\delta$ TnpR, Tn*501* TnpR	—	—	—	1
Piv/IS*110*	DED/DDD	IS *110*, IS*492*	Piv	—	—	—	—	3
RAG	DDE?*	RAG-1 RAG-2	—	—	—	—	RAG-1 RAG-2	4, 38, 39
DNA Tpase/ retroviral integrase	DDE	IS*2*, Tn*10*, IS*911*, *Tn*3* TnpA	—	—	HIV-1 Int, RSV Int	—	—	1
IS*30*†	DDE	IS*30* Tpase	IS*30* Tpase	IS*30* Tpase	IS*30* Tpase	IS*30* Tpase‡	—	This work, 15

*Spacing between D and D and E amino acids differs from that of classical DDE motif of Tpase/integrase family.
†IS*30* family Tpases are members of the classical DDE Tpase/integrase family. This row represents which types of functions the IS*30* Tpase could fulfill in different experimental situations.
‡Integron-like functioning of an IS*30*-based system is described in ref. 15.

to catalyze site-specific recombination. This finding may provide support for the theory that evolution of primitive recombinases can lead to the development of enzyme families, which can accomplish both transpositional and site-specific rearrangements independent of their catalytic mechanism.

We thank H. Ikeda for λ *red*113 cI857; I. Könczöl, E. Keresztúri, and M. Turai for skillful technical assistance; and K. Schlett for critical reading of the manuscript. This work was supported by Ministry of Education Grant NKFP4/006 and Hungarian National Scientific Research Foundation (Országos Tudományos Kutatási Alapprogramok) Grants T019365 and T025729 (to F.O.) and F038204 (to J.K.).

1. Craig, N. L., Craigie, R., Gellert, M. & Lambrowitz, A. M., eds. (2002) *Mobile DNA II* (Am. Soc. Microbiol., Washington, DC).
2. Choi, S., Ohta, S. & Ohtsubo, E. (2003) *J. Bacteriol.* **185,** 4891–4900.
3. Tobiason, M., Buchner, J. M., Thiel, W. H., Gernert, K. M. & Karls, A. C. (2001) *Mol. Microbiol.* **39,** 641–651.
4. Oettinger, M. A. (1999) *Curr. Opin. Cell Biol.* **11,** 325–329.
5. Nunes-Düby, S. E., Kwon, R. S., Tirumalai, H. J., Ellenberger, T. & Landy, A. (1998) *Nucleic Acids Res.* **26,** 391–406.
6. Lenich, A. G. & Glasgow, A. C. (1994) *J. Bacteriol.* **176,** 4160–4164.
7. Reimmann, C. & Haas, D. (1987) *Genetics* **115,** 619–625.
8. Olasz, F., Stalder, R. & Arber, W. (1993) *Mol. Gen. Genet.* **239,** 177–187.
9. Turlan, C., Ton-Hoang, B. & Chandler, M. (2000) *Mol. Microbiol.* **35,** 1312–1325.
10. Szeverényi, I., Nagy, Z., Farkas, T., Olasz, F. & Kiss, J. (2003) *Microbiology* **149,** 1297–1310.
11. Mahillon, J. & Chandler, M. (1998) *Microbiol. Mol. Biol. Rev.* **62,** 725–774.
12. Dalrymple, B., Caspers, P. & Arber, W. (1984) *EMBO J.* **3,** 2145–2149.
13. Olasz, F., Farkas, T., Kiss, J., Arini, A. & Arber, W. (1997) *J. Bacteriol.* **179,** 7551–7558.
14. Olasz, F., Kiss, J., König, P., Buzás, Z., Stalder, R. & Arber, W. (1998) *Mol. Microbiol.* **28,** 691–704.
15. Kiss, J. & Olasz, F. (1999) *Mol. Microbiol.* **34,** 37–52.
16. Stalder, R. & Arber, W. (1989) *Gene* **76,** 187–193.
17. Szeverényi, I., Hodel, A., Arber, W. & Olasz, F. (1996) *Gene* **174,** 103–110.
18. Dalrymple, B. (1987) *Mol. Gen. Genet.* **207,** 413–420.
19. Prentki, P. & Krisch, H. M. (1984) *Gene* **29,** 303–313.
20. Boyer, H. W. & Roulland-Dussoix, D. (1969) *J. Mol. Biol.* **41,** 459–472.
21. Sambrook, J., Fritsch, E. F. & Maniatis, T. (1989) *Molecular Cloning: A Laboratory Manual* (Cold Spring Harbor Lab. Press, Plainview, NY).
22. Dente, L., Cesareni, G. & Cortese, R. (1983) *Nucleic Acids Res.* **11,** 1645–1655.
23. Arini, A., Keller, M. P. & Arber, W. (1997) *Biol. Chem.* **378,** 1421–1431.
24. Herrero, M., Lorenzo, V. & Timmis, K. N. (1990) *J. Bacteriol.* **172,** 6557–6567.
25. Johnson, R. C. (2002) in *Mobile DNA II*, eds. Craig, N. L., Craigie, R., Gellert, M. & Lambrowitz, A. M. (Am. Soc. Microbiol., Washington, DC), pp. 230–271.
26. Summers, D. K., Beton, C. W. H. & Withers, H. L. (1993) *Mol. Microbiol.* **8,** 1031–1038.
27. Hoess, R. H. & Abremski, K. (1984) *Proc. Natl. Acad. Sci. USA* **81,** 1026–1029.
28. Kuempel, P. L., Henson, J. M., Dircks, L., Tecklenburg, M. & Lim, D. F. (1991) *New Biol.* **3,** 799–811.
29. Plasterk, R. H., Ilmer, T. A. & Van de Putte, P. (1983) *Virology* **127,** 24–36.
30. Haffter, P. & Bickle, T. A. (1988) *EMBO J.* **7,** 3991–3996.
31. Sandmeier, H., Iida, S., Meyer, J., Hiestand-Nauer, R. & Arber, W. (1990) *Proc. Natl. Acad. Sci. USA* **87,** 1109–1113.
32. Koch, C. & Kahmann, R. (1986) *J. Biol. Chem.* **261,** 15673–15678.
33. Szeverényi, I., Bodoky, T. & Olasz, F. (1996) *Mol. Gen. Genet.* **251,** 281–289.
34. Iida, S., Huber, H., Hiestand-Nauer, R., Meyer, J., Bickle, T. A. & Arber, W. (1984) *Cold Spring Harbor Symp. Quant. Biol.* **49,** 769–777.
35. Weisberg, R. A. & Landy, A. (1983) in *Lambda II*, eds. Hendrix, R. W., Roberts, J. W., Stahl, F. W. & Weisberg, R. A. (Cold Spring Harbor Lab. Press, Plainview, NY), pp. 211–250.
36. Caspers, P., Dalrymple, B., Iida, S. & Arber, W. (1984) *Mol. Gen. Genet.* **196,** 68–73.
37. Umeda, M. & Ohtsubo, E. (1990) *Mol. Gen. Genet.* **222,** 317–322.
38. Li, W., Chang, F. C. & Desiderio, S. (2001) *Mol. Cell. Biol.* **21,** 3935–3946.
39. van Gent, D. C., Mizuuchi, K. & Gellert, M. (1996) *Science* **271,** 1592–1594.